

Targeting EZH2 for glioma therapy with a novel nanoparticle–siRNA complex

This article was published in the following Dove Medical Press journal:
International Journal of Nanomedicine

Xiang Wang¹
Yuanqi Hua¹
Guangya Xu¹
Senyi Deng¹
Daoke Yang²
Xiang Gao¹

¹Department of Neurosurgery, Institute of Neurosurgery, State Key Laboratory of Biotherapy, West China Hospital, West China Medical School, Sichuan University, Collaborative Innovation Center for Biotherapy, Chengdu 610041, China; ²Tumor Hospital of First Affiliated Hospital of Zhengzhou University, Zhengzhou 450052, China

Background: For the past few years, gene-therapy has recently shown considerable clinical benefit in cancer therapy, and the applications of gene therapies in cancer treatments continue to increase perennially. EZH2, an ideal candidate for tumor gene therapy, plays an important role in the tumorigenesis.

Methods: In this study, we developed a novel gene delivery system with a self-assembly method by Methoxy polyethylene glycol-polycaprolactone (MPEG-PCL) and DOTAP(DMC). And EZH2si-DMC was used to research anti-glioma both in vitro and in vivo.

Results: DMC with zeta-potential value of 36.7 mV and size of 35.6 nm showed good performance in the delivery siRNA to glioma cell in vitro with high 98% transfection efficiency. EZH2si-DMC showed good anti-glioma effect in vitro through inducing cell apoptosis and inhibiting cell growth. What's more, treatment of tumor-bearing mice with DMC-EZH2si complex had significantly inhibited tumor growth at the subcutaneous model in vivo by inhibiting EZH2 protein expression, promoting apoptosis and reducing proliferation.

Conclusion: The EZH2 siRNA and DMC complex may be used to treat the glioma in clinical as a new drug.

Keywords: glioma, gene therapy, EZH2, MPEG-PCL, DOTAP, tumorigenesis

Introduction

The patient who suffered from grade IV glioblastoma (GBM) had the highest death rate.^{1,2} Surgery, chemotherapy and radiotherapy were used to treat glioma patients, which improve the quality of life of glioma patients at a certain degree.³ The average survival of glioblastoma patients is only 12–15 months, as the unclear boundaries between the tumor and normal tissue leads to unclearly removal tumor by surgery and the tumor tolerance to the chemotherapy.⁴ Hence, finding a new method for glioma therapy is of interest. Although it was well known that cancer is caused by the gene regulation for several years, the concern about specific target gene is still inadequate.

Currently, many cancer-associated genes are identified such as *EZH2*, *PRMT5* and *SMYD3*. *EZH2* is the central active subunit of the PRC2 complex that includes the following three subunits: EED, SUZ12 and RbAp46/48. PRC2 can cause 27-lysine of histone 3 (H3K27) methylation, and this process can make the chromosome close, leading to gene silencing.^{5–7} H3K27 methylation has been correlated with transcriptional repression and heterochromatin formation.⁸ In mammals, *EZH2* gene has a relatively high expression in stem cells and actively proliferative cells but low expression in differentiation cells.⁹ A number of studies had shown that *EZH2* is overexpressed in many tumors such as prostate cancer, breast cancer, liver cancer and others, and reducing the expression of *EZH2* in tumor cells could inhibit proliferation, migration, invasion, angiogenesis and induce apoptosis.^{10–13}

Correspondence: Xiang Gao
Department of Neurosurgery,
Institute of Neurosurgery, State Key
Laboratory of Biotherapy, West China
Hospital, West China Medical School,
Sichuan University, Collaborative
Innovation Center for Biotherapy, No.3
Middle Section of People South Road,
Chengdu 610041, China
Tel +86 28 8542 2136
Fax +86 28 8550 2796
Email xianggao@scu.edu.cn

Gene therapy is an emerging treatment for various diseases such as cancer and autoimmune diseases.¹⁴ RNA interference (RNAi) is a homologous RNA degradation process by double-stranded RNA, which is found in the process of studying the antisense RNA of *Caenorhabditis elegans* (antisense RNA). siRNA consists of a double-stranded RNA of 20–25 nucleotides, which knocks down the specific target gene by degrading the mRNA and inhibiting the production of the relative protein. It is known that siRNA is mainly involved in RNAi phenomenon, with a specific way to regulate gene expression.

Although siRNA has shown enormous potential as a therapeutic strategy, the delivery of specific gene sequences to target cells is still confronted with great challenges on account of nuclease degradation and low cellular uptake in vivo. Consequently, it is very important to use a safe and non-toxic effective delivery system.

Clinical application of gene therapy is limited due to the lack of effective and safe gene transfer technology. Commercially available branched polyethylenimine (PEI; 25,000 kDa, PEI25k), an effective non-viral gene transfection agent, has been applied as a “gold standard” to estimate the transfection efficiency of other newly developed non-viral gene vectors.^{15–18} But, PEI could not be biodegraded and has grave cytotoxicity, and thus finding an effective gene delivery system is very meaningful. MPEG-PCL is a biodegradable and very safe polymer, and so it was chosen as a framework system. In this research, we prepared biodegradable DMC nanoparticles as a novel non-viral gene carrier, which has low cytotoxicity and high transfection efficiency. DMC nanoparticles delivering EZH2 siRNA were used to treat glioma in vitro and in vivo, and their antiglioma effect was assessed.

Materials and methods

Materials

1,2-Dioleoyl-3-trimethylammonium-propane (DOTAP) (chloride salt) was provided by Avanti Polar Lipids Inc. (Alabaster, AL, USA). MTT was obtained from Sigma-Aldrich Co. (St Louis, MO, USA). DMEM and FBS were purchased from Thermo Fisher Scientific (Waltham, MA, USA). Methanol and acetic acid (HPLC grade) were acquired from Thermo Fisher Scientific. Dimethyl sulfoxide (DMSO) and acetone were approved by KeLong Chemicals (Chengdu, China). Antibodies were purchased from Abcam (Cambridge, UK), consisting of rat anti-mouse CD31 polyclonal antibody (BD Pharmingen™; BD, Franklin Lake, NJ, USA), rabbit anti-mouse Ki67 antibody (Abcam) and rhodamine-conjugated secondary antibody.

MPEG(2,000)-PCL(2,000) diblock copolymer was synthesized by ring opening of ϵ -caprolactone initiated by MPEG and had the molecular weight of 4,000 Da. First, 5.0 g MPEG, 5.0 g anhydrous ϵ -caprolactone and Sn(Oct)₂ were dissolved in a 50 mL flask under nitrogen at 125°C for 24 hours. The product was dissolved in tetrahydrofuran, then filtrated and purified by ice-cooled diethyl ether. The resultant product was vacuum dried at ambient temperature, and the average molecular weight of the MPEG-PCL copolymer was 4,010 Da.

Preparation of DMC nanomicelles

DMC was synthesized using a self-assembly method. First, 10 mg DOTAP and 90 mg MPEG-PCL were dissolved in acetone. The acetone was removed under negative pressure conditions, and 5% glucose water solution was added. Finally, the DMC nanomicelles were successfully prepared and stored at 4°C for future use.

Characterization of DMC nanomicelles

The transmission electron microscope (TEM; H-6009IV; Hitachi Ltd., Tokyo, Japan) was employed to observe the morphology of DMC. The nanoparticles were placed on a copper grid covered with nitrocellulose after diluting with distilled water and then stained negatively with phosphotungstic acid. The particle size and zeta potential of DMC nanoparticles were measured by dynamic light scattering (Nano-ZS 90; Malvern Instruments, Malvern, UK) under 25°C temperature conditions.

Preparation of siRNA-DMC complexes

DMC-siRNA complexes were prepared by mixing 5 μ g DMC (1 μ L, 5 mg/mL) solution with 0.1 nm siRNA, followed by incubation for 30 minutes at room temperature.

The siRNA-DMC complexes with different weight ratios ranging from 1:10 to 1:50 (siRNA:DMC) were electrophoresed in a 2% (w/v) agarose gel at 150 V for 30 minutes. Then, the agarose gel was stained with ethidium bromide (0.5 mg/mL) and illuminated on an UV illuminator to reveal the location of RNA.

Transfection in vitro

The U87 cells and GL261 (purchased from American Type Culture Collection, Manassas, VA, USA) were seeded at the density of 3×10^5 /well in six-well plates with 2 mL complete DMEM containing 10% fetal calf serum for 24 hours, and then the medium was replaced with 1 mL fresh serum-free

DMEM at the time of transfection. Fluorescein isothiocyanate (FITC)-labeled siRNA (siRNA-FITC) was applied as a reporter gene, and the amount of siRNA was kept at 0.1 nm/well, while the weight ratios of DMC/SiRNA-FITC were 5/1, 25/1, and 50/1, respectively. The fluorescence microscope (Carl Zeiss Meditec AG, Jena, Germany) and flow cytometry (Epics Elite ESP; Beckman Coulter, Fullerton, CA, USA) were employed to observe the transfected cells and evaluate the transfection efficiency.

MTT assay

The U87 cells were seeded at the density of 5×10^3 /well in 96-well plates with 100 μ L complete DMEM containing 10% fetal calf serum for 24 hours, and then the medium was replaced with fresh serum-free DMEM at the time of transfection. EZH2 siRNA (siEZH2-1: GGATACAGCCTGTGCACAT; siEZH2-2: GCTCTAGACAACAAACCTT; siEZH2-3: GCAGCTTTCTGTTCAACTT) was applied as a reporter gene, and the amount of siRNA was kept at 0.01 nm/well, while the weight ratio of DMC/siRNA was 50/1. The MTT assay was performed to study the cell cytotoxicity, and the absorbance was evaluated by the plate reader.

Cell apoptosis test

U87 cells were seeded on six-well plates (Corning Incorporated, Corning, NY, USA) at a density of 3×10^5 cells per well with DMEM medium. After 24 hours, U87 cells were transfected with DMC, DMC-Consi or DMC-EZH2si (siEZH2-1: GGATACAGCCTGTGCACAT; siEZH2-2: GCTCTAGACAACAAACCTT; siEZH2-3: GCAGCTTTCTGTTCAACTT), or treated with glucose solution (GS) as a negative control. After 72 hours, flow cytometry (FCM; FACSCalibur; BD Biosciences, San Jose, CA, USA) was used to assess the extent of apoptosis in U87 cells by the FITC-conjugated Annexin V/propidium iodide (PI) staining according to the manufacturer's instructions, and the early and late apoptotic cells were all detected.

Western blot

The Western blot assay was performed to detect the expression level of EZH2 protein in U87 cells. The U87 cells washed with cold PBS were lysed in RIPA buffer containing 1 mM phenylmethyl sulfonyl fluoride and 2 μ g/mL protease inhibitors for 30 minutes, and then the cell lysate was centrifuged at $12,000 \times g$ for 15 minutes. The supernatant was collected, and the Lowry method was used to measure the protein content. First, 2 μ g of each sample

was electrophoresed on a 10% SDS-PAGE gel at 120 V for 60 minutes, and then was transferred to the polyvinylidene difluoride membrane at 100 V for another 60 minutes. The specific protein was detected by primary antibody treatment with rabbit anti-EZH2 (1:1,000 dilution; CST, Boston, MA, USA) and rabbit anti- β -actin (1:1,000 dilution; CST) overnight at 4°C and secondary antibody treatment with HRP-conjugated goat anti-rabbit IgG antibody (1:5,000 dilution) for 2 hours at room temperature using an ECL kit (SignaGen, Jinan, China). The membranes were then probed with primary antibody against Bax, Bcl-2, Akt, p-Akt, MAPK, p-MAPK and β -actin followed by incubation with secondary antibodies.

Xerographic tumor model

All animal experiments were performed in accordance with the guidelines and approved by the Animal Care Committee of Sichuan University (Chengdu, China). The animal model was established by female nude BALB/c mice, and the U87 cell suspension (100 μ L) at a density of 1×10^7 was injected subcutaneously into the right flank. When the mean diameter of the tumors was about 6 mm, all the tumor-bearing mice were randomly divided into four groups as follows: normal saline, DMC nanoparticles (25 μ g), ConsiRNA DMC complexes (1 nm siRNA/100 μ g DMC) and EZH-2 siRNA-DMC complexes (1 nm siRNA/100 μ g DMC). The mice were treated by intratumoral injection with ten doses once 2 days. The tumor volume was calculated as $0.52 \times \text{length} \times \text{width}^2$ and recorded every 3 days. When the mice in the control group became very weak, all were sacrificed by dislocation of the cervical vertebra.

In addition, the mice orthotopic glioma model was built for better simulation of site-specific pathology of glioma. Female C57/BL6 mice (age, 6–8 weeks) were fed with regular diet and housed in top-filtered cages in animal research laboratory of Sichuan University. GL261 cells were infected with luciferase lentivirus. All mice were implanted with GL261 cells under sterile conditions in accordance with the well-established protocol in our institution. Briefly, animal was fixed in a stoelting stereotaxic Instrument stereotactic head frame in a prone position after anesthetization with intraperitoneal injection of phenobarbital. A vertical incision was performed to expose the coronal suture. Next, a burr hole was made 1 mm anterior to the coronal suture and 1 mm right to the middle line. Five microliters of GL261 cell solution at a concentration of 2×10^5 cells/mL were injected 3 mm deep into brain over 5 minutes with needle (10 μ L, Neuros Model 1701 RN, point style 4, SYR, Bonaduz, Switzerland).

Then, the needle was removed, the burr hole was closed with bone wax, and the incision was sutured. After 7 days, they were treated with normal saline, DMC nanoparticles (25 μg), ConsiRNA DMC complexes (1 nm siRNA/100 μg DMC) and EZH-2 siRNA-DMC complexes (1 nm siRNA/100 μg DMC) through intracranial injection every day. Images were captured using the in vivo imaging system heated to 37°C (Quick View 3000) 2 weeks after implantation. The survival time in different groups was recorded for comparison.

Analysis of apoptosis and proliferation in vivo

The tumor tissues were fixed and embedded by paraformaldehyde and paraffin, and then cut into cross-sections about 3–5 μm thick. The sections were dealt with TUNEL kit (Promega Corporation, Fitchburg, WI, USA) to detect the apoptotic cells in the tumors by the fluorescence microscope (400 \times).

Meanwhile, a part of the tumor tissues were stored at -80°C and immunostained with rabbit anti-human ki67 antibody (dilution 1:100; Abcam) overnight at 4°C to examine the cell proliferation. Goat-antirabbit tetraethyl rhodamine isothiocyanate (TRITC) (dilution 1:100; Santa Cruz Biotechnology Inc., Dallas, TX, USA) was co-incubated at 37°C for 1 hour and counterstained with Hoechst 33258 for 10 minutes, and then the sections were observed using fluorescence microscope.

Drug toxicity evaluation

The blood was collected from the eyeball of mice 24 hours after injection of agents for evaluation of drug toxicity through blood routine test (BRT) and blood biochemical test (BBT). The group injected with normal saline was used as a control. Next, we sacrificed the mice and collected organs

for further histology examination under a microscope using HE staining. Images were captured for observation.

Statistical analyses

The GraphPad Prism software (GraphPad Software, Inc., La Jolla, CA, USA) was used to analyze all the data. The data from multiple groups and the multiple comparisons between groups were analyzed by ANOVA and Newman–Keuls method. Survival data were plotted by Kaplan–Meier curves and analyzed using the log-rank test. Tumor volumes [(smaller diameter)²(larger diameter) \times 0.52] were analyzed using Student's *t*-test. All values were presented as mean \pm standard error of measurement, and $*P < 0.05$ was considered to be statistically significant.

Results

Preparation and characterization of the DMC

The DMC was prepared by a self-assembly method and consisted of MPEG-PCL and DOTAP, with a spherical shape (Figure 1). As shown in Figure 2A and B, the size and zeta potential of DMC were 34.67 nm and 36 mV, respectively. TEM images show that, morphologically, DMC adopts a bilayer spheroidal structure at around 26 nm in diameter (Figure 2C). Gel retardation assays were used to characterize the ability of the DMC to carry siRNA. As shown in Figure 2D, free siRNA not entrapped in the DMC appeared as a bright band (lanes 2–4) (weight ratio of DMC/siRNA: lane 3:10:1; lane 4:25:1), and no other band of free siRNA was observed from lanes 5 to 6 (weight ratio of DMC/siRNA: lane 5:50:1; lane 6:100:1). This suggests that siRNA was completely incorporated into the DMC and that the complexes

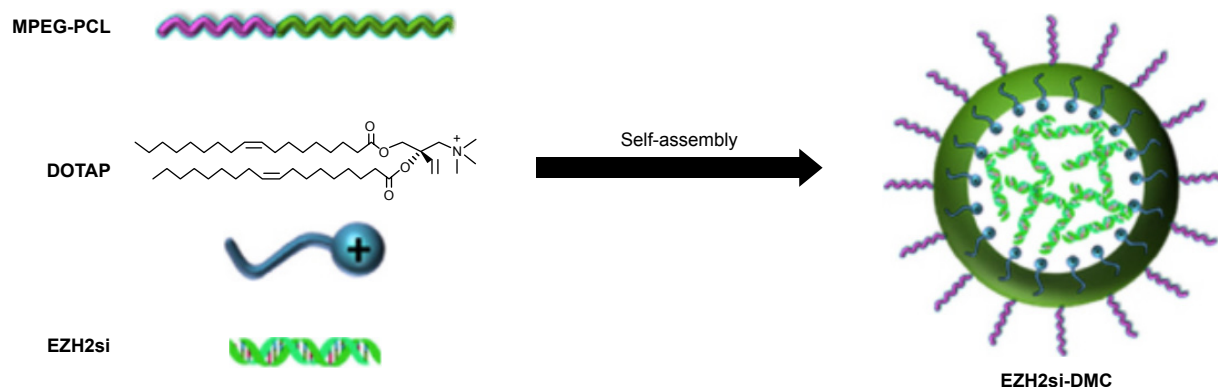


Figure 1 Preparation of DMC.

Notes: Preparation of DMC and EZH2si complex: first, a novel gene carrier was prepared by a self-assembly method. MPEG-PCL and DOTAP were assembled into a new gene carrier, DOTAP/MPEG-PCL micelles (DMC). Then, EZH2 siRNA was carried into cancer cells by DMC.

Abbreviation: DOTAP, 1,2-dioleoyl-3-trimethylammonium-propane.

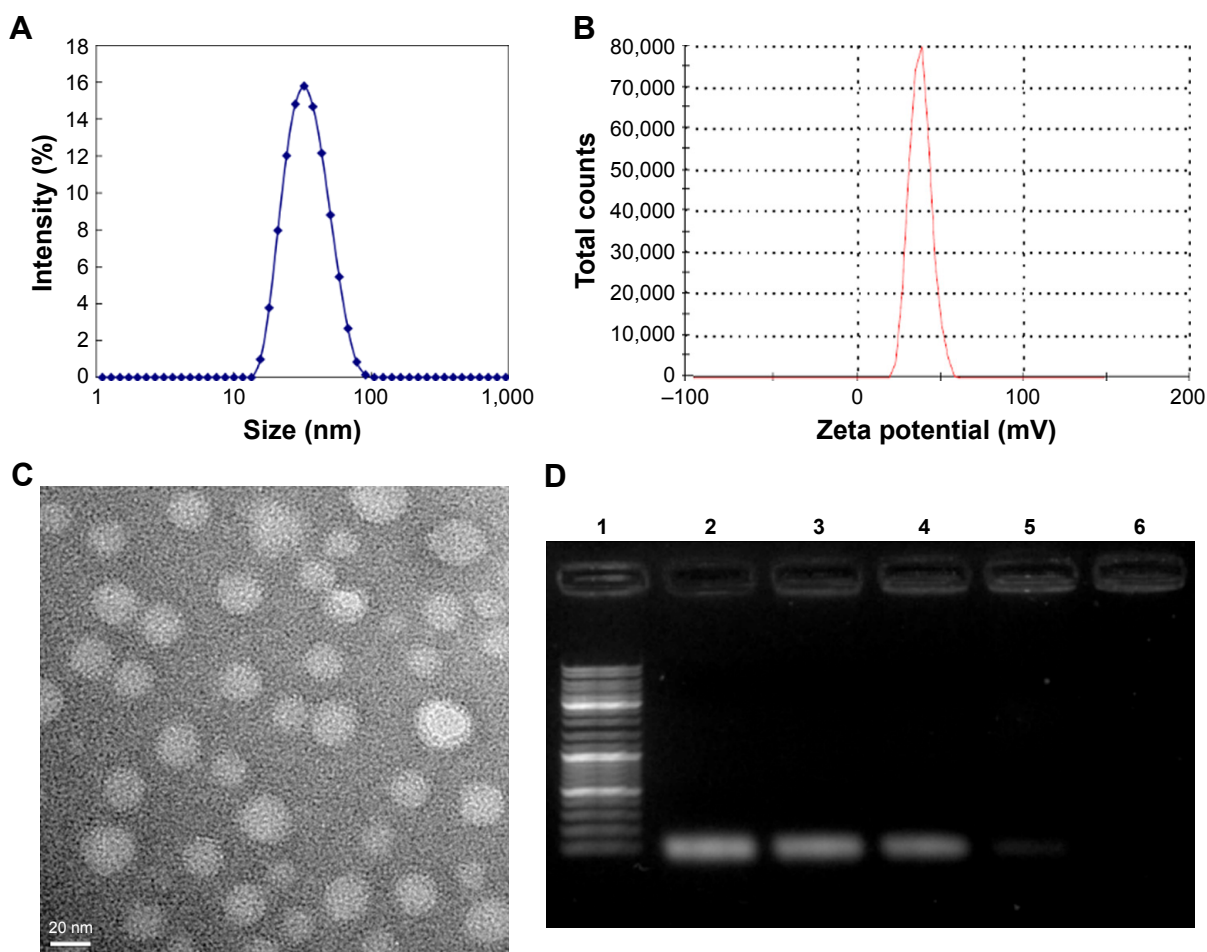


Figure 2 Physicochemical properties of DMC.

Notes: (A) Particle size of DMC; (B) zeta potential of DMC; (C) morphological characteristics of DMC by TEM observation; and (D) gel retardation assay of siRNA and complexes. Lane 1, DNA marker; lane 2, naked siRNA; lanes 3–6, different weight ratios of siRNA with DMC. siRNA was completely incorporated into DMC at a weight ratio of 1:50, and complexes were prepared without free siRNA.

Abbreviation: TEM, transmission electron microscope.

were prepared successfully without free siRNA at the weight ratio of 50 times the amount of DMC to siRNA.

DMC-siRNA has high transfection efficiency in U87 cells

In the cell transfection assays *in vitro*, DMC had high transfection efficiency in U87 cells after incubation for 4 hours as shown in Figure 3A. The specific transfection rates demonstrated by flow cytometry analysis were 79.2%, 92% and 94.4% when DMC was mixed with FITC-siRNA at a ratio of 1:50, 1:100 and 1:150, respectively (Figure 3B).

EZH2si-DMC causes antitumor effects *in vitro*

U87 cells were transfected with DMC, Consi-DMC or EZH2si-DMC. After 48 hours, we then measured the expression of

EZH2 in these group cells by reverse transcription PCR (RT-PCR) and Western blot (Figures 4A, B and S1A). We found that the expression of EZH2 was decreased in the EZH2si-DMC treatment group. Furthermore, cell activity of those groups was detected by MTT. The result showed that the cell activity in the EZH2si-DMC group was lower than other groups (Figures 4C and S1B). Finally, the cell apoptosis was detected by Annexin-FITC/PI staining with flow cytometry analysis. The cell apoptosis rates of EM-DMC, Consi and EZH2si groups are 4.5%, 5.3% and 27%, respectively (Figure 5).

Molecular mechanism

To investigate the mechanism of the anticancer effect of EZH2si-DMC, protein expressions related to cell apoptosis and proliferation following treatment of EZH2si-DMC, Consi-DMC and DMC were examined. As demonstrated in

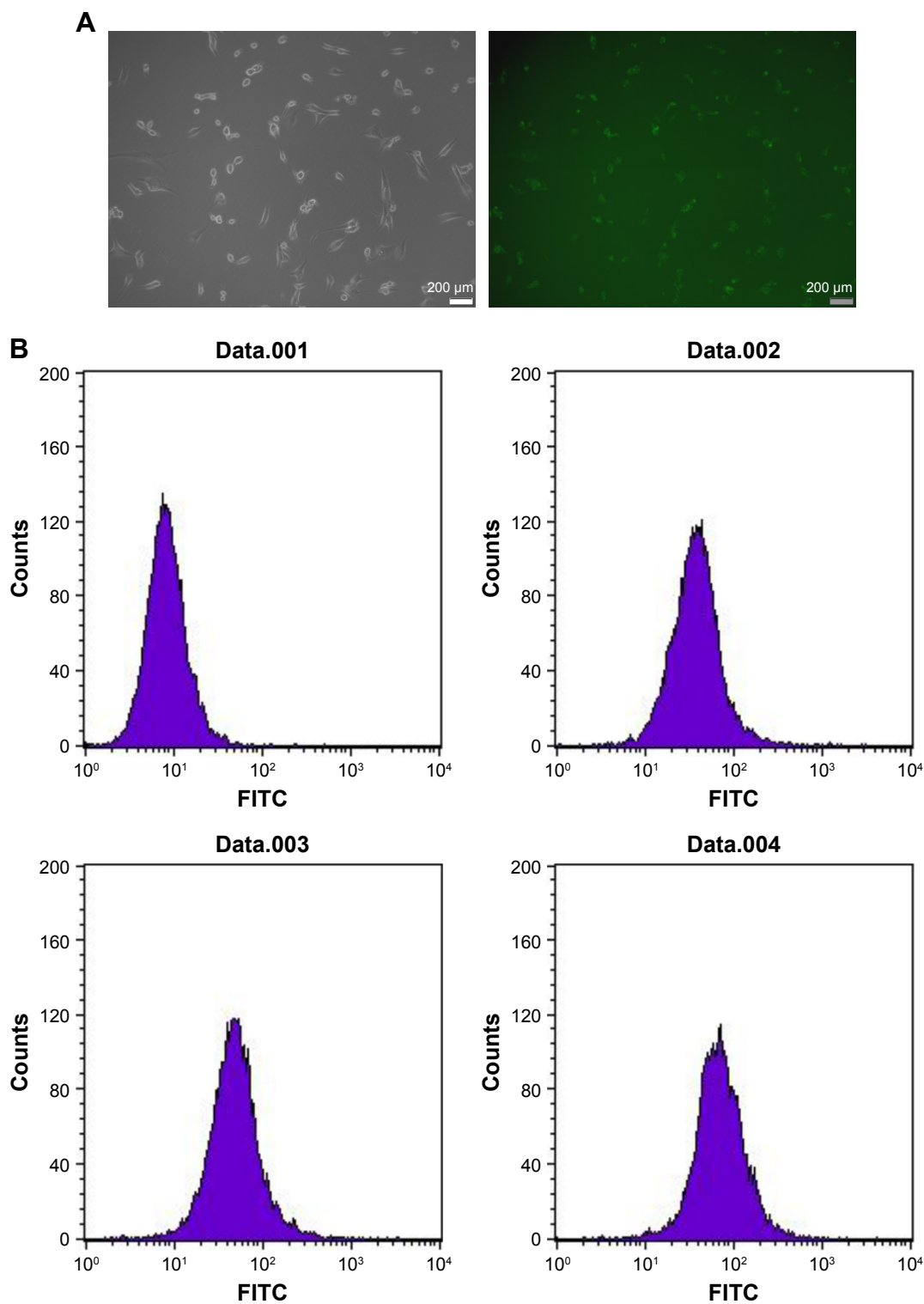


Figure 3 Transfection efficiency measurement of DMC.

Notes: DMC, containing 4 μg siRNA, was used to transfect U87 cells for 4 hours. The transfection efficiencies at both weight ratios (siRNA vs DMC as 1:100 and 1:150) were determined using (A) fluorescence microscope and (B) flow cytometry.

Abbreviation: FITC, fluorescein isothiocyanate.

Figure 6, the Bcl-2 protein expression was decreased and the Bax expression increased after EZH2si-DMC treatment, indicating that EZH2si-DMC induced apoptosis through the mitochondrial pathway. Finally, the levels of MAPK and

p-MAPK after EZH2si-DMC treatment were also tested, and the result showed that p-MAPK and p-Akt were obviously decreased after 72-hour treatment with EZH2si-DMC, whereas the total MAPK and Akt were unchanged.

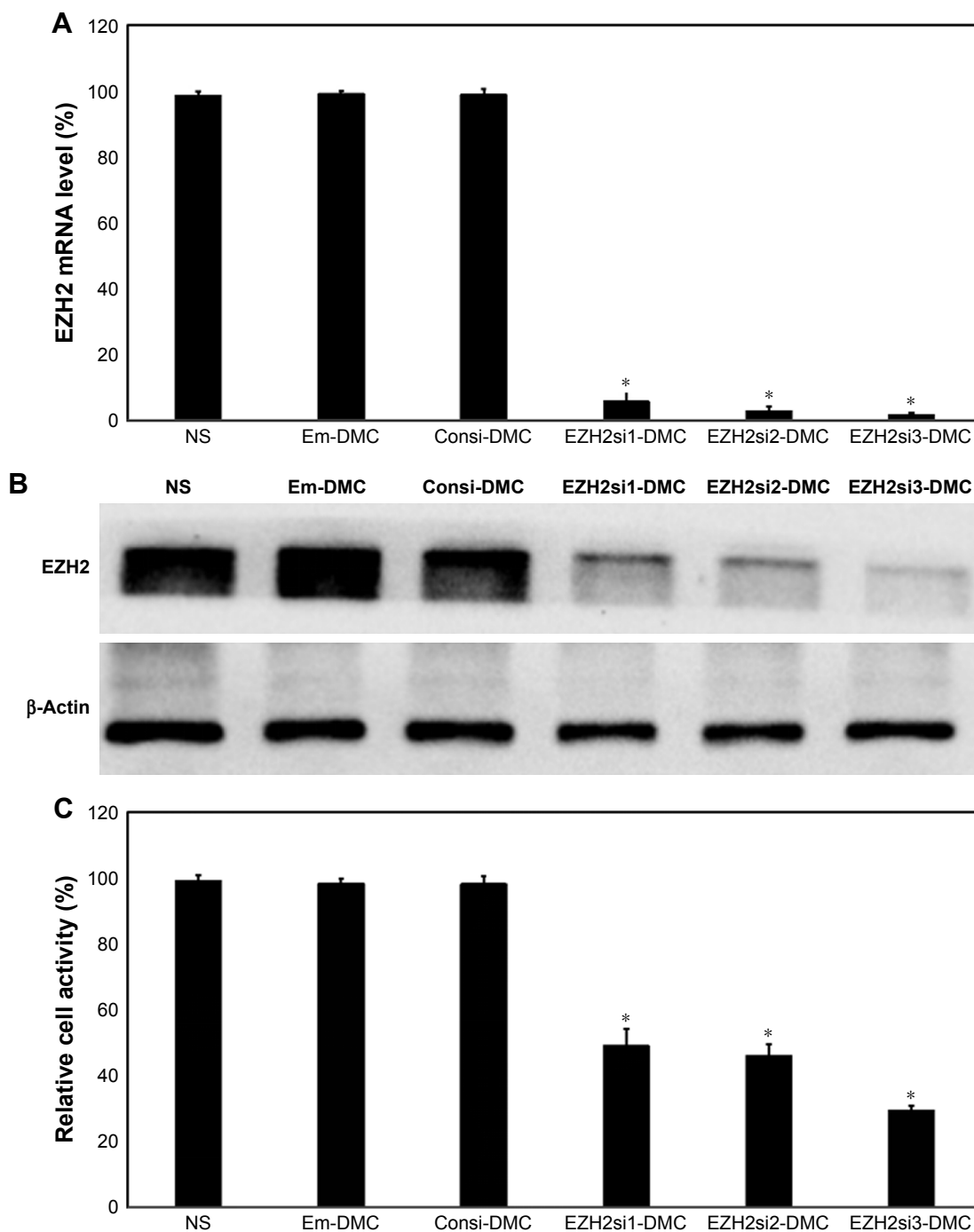


Figure 4 RT-PCR, Western blot and MTT test of cell activity.

Note: When U87 cells were transfected with DMC, Consi-DMC or EZH2si-DMC for 72 hours, EZH2 expression was tested by RT-PCR (A) and Western blot (B), and cell activity was tested by MTT test (C). * $P < 0.01$, EZH2si-DMC versus NS, DMC, Consi-DMC.

Abbreviations: RT-PCR, reverse transcription PCR; NS, normal saline.

EZH2si-DMC causes antitumor effects in vivo

DMC and its complexes loaded with Consi and EZH2si were used to treat U87 glioma in a nude BALB/c mice model via intratumor injection. EZH2si-DMC treatment showed dramatic antitumor effects than other complexes (Consi-DMC, DMC and normal saline [NS]) as shown in Figure 7A–C,

and no significant differences were observed among mice in the Consi-DMC, DMC and NS groups. In addition, EZH2si-DMC-treated mice had no significant changes in body weight compared with mice in the control groups (Figure 7D).

In the mice orthotopic glioma model, mice were treated with normal saline, DMC nanoparticles (25 μ g), ConsiRNA DMC complexes (1 nm siRNA/100 μ g DMC) and EZH2si-DMC

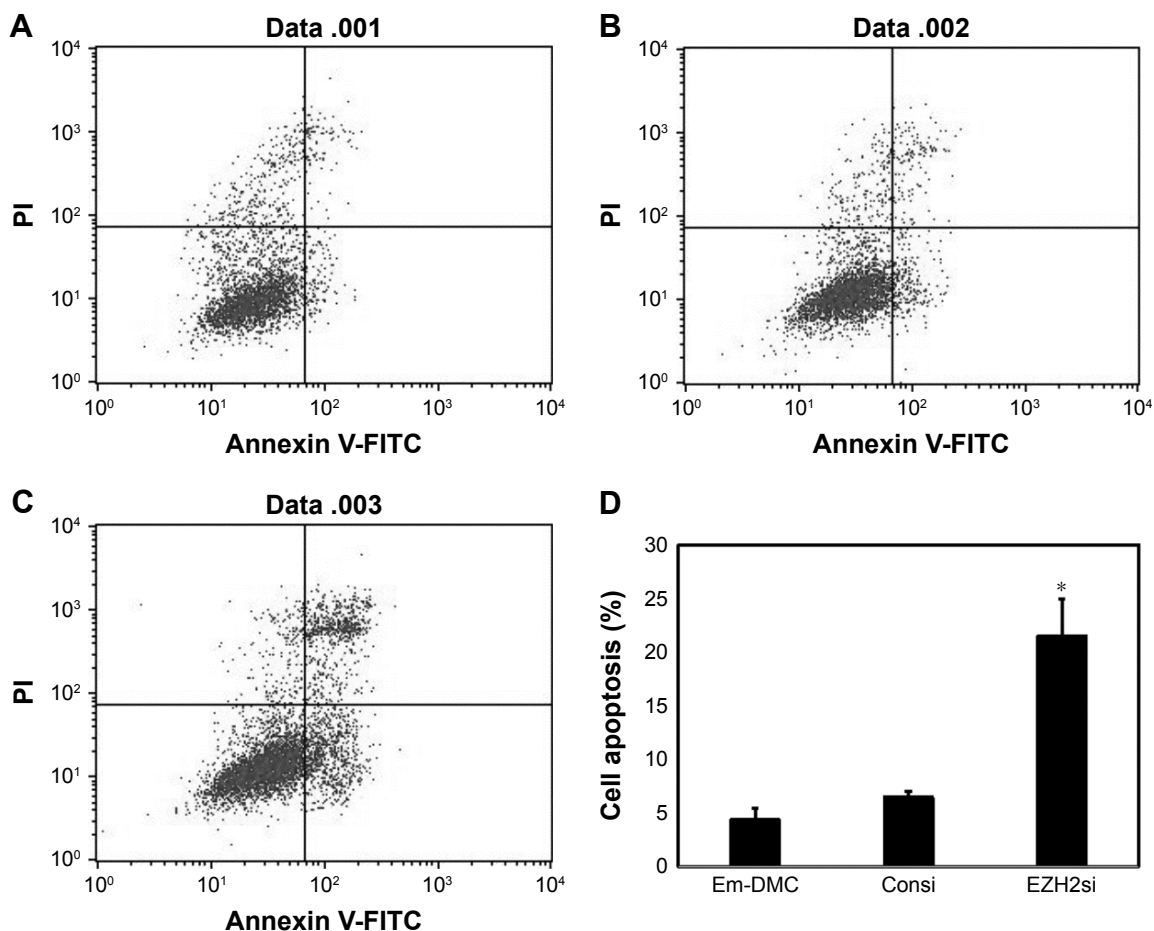


Figure 5 Cell apoptosis test.

Notes: When U87 cells were transfected with DMC (A), Consi-DMC (B) or EZH2si-DMC (C) for 72 hours, U87 cells with different treatments were stained with Annexin V-FITC/PI and tested by flow cytometry. (D) Statistics of tumor cell apoptosis. * $P < 0.05$.

Abbreviations: FITC, fluorescein isothiocyanate; PI, propidium iodide.

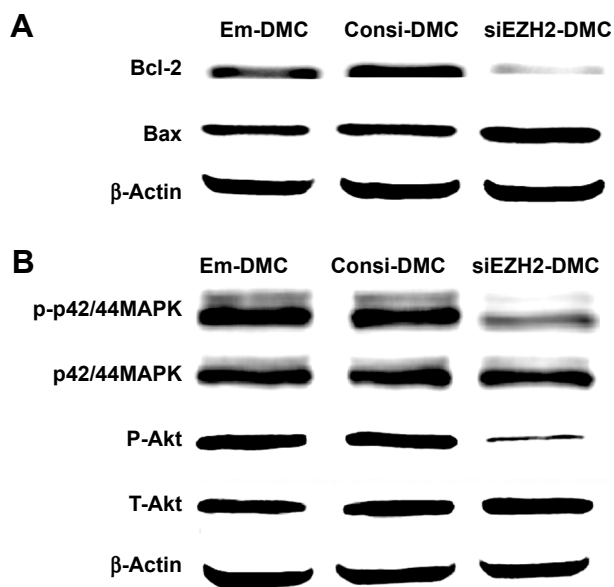


Figure 6 Molecular mechanism of siEZH2-DMC antiglioma.

Notes: (A) The effect of siEZH2-DMC on apoptosis-related proteins by Western blotting analysis. (B) The phosphorylation of Akt and p44/42 MAPK in U87 was inhibited by siEZH2-DMC.

complexes (1 nm siRNA/100 μ g DMC) 2 weeks after implantation and were observed using the bioimaging system (Figure 8). It is obvious that EZH2si-DMC complexes inhibited tumor growth more efficiently than others, and tumor emitting fluorescence is the smallest in four groups, since the life span of mice in the EZH2si-DMC complexes group is the longest.

EZH2si-DMC induces apoptosis of cancer cells and inhibits tumor cell proliferation in vivo

Antitumor mechanisms of EZH2si-DMC were studied by EZH2 staining, TUNEL and Ki67 staining. The EZH2si-DMC treatment group also showed that the expression of EZH2 was knocked down in tumors compared to DMC-Consi, DMC and NS as determined by EZH2 staining (Figure 9). Furthermore, compared to other groups measured by TUNEL assay, the group treatment with EZH2si-DMC had a significant increase of apoptosis in the tumor cells

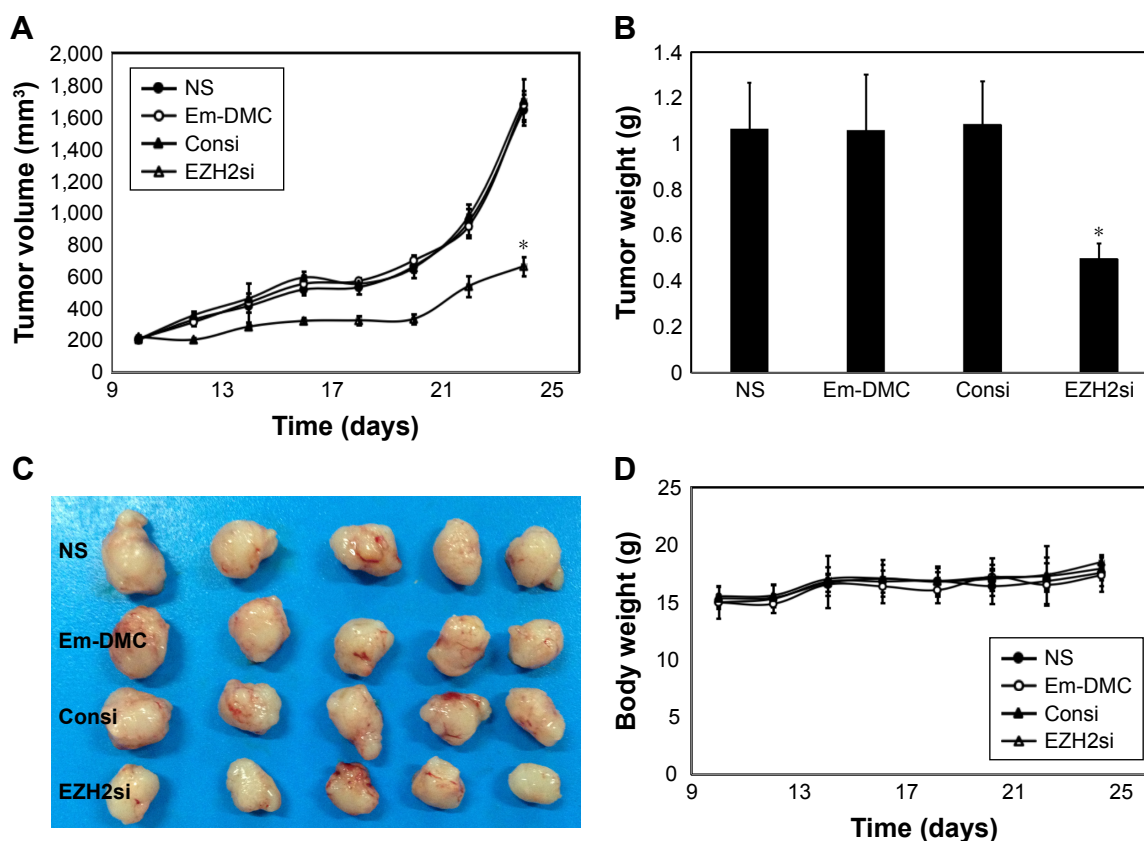


Figure 7 Antiglioma effect of EZH2si-DMC in vivo.

Notes: (A) Tumor growth curves; (B) tumor weight; (C) tumor photos of NS, DMC, DMC-Consi and DMC-EZH2si treatment groups; and (D) body weight of different groups. (Mean \pm SEM, n=5) (* P <0.01, DMC-EZH2si vs NS, DMC, DMC-Consi (A); * P <0.01, DMC-EZH2 vs NS, DMC, and DMC-Consi (B).

(Figure 10). In addition, EZH2si-DMC could inhibit proliferation of tumor cells. Treatment with EZH2si-DMC significantly inhibits cancer cell proliferation compared to other groups as determined by Ki67 staining (Figure 11). These results suggested that EZH2si-DMC induced apoptosis of glioma, inhibited glioma cell proliferation, thus causing the antitumor effects observed in this study.

EZH2si-DMC has no toxicity

Tissue sections from internal organs, including heart, liver, spleen, lung and kidney, were stained with HE and examined under a microscope. As shown in Figure S2, tissue sections of vital organs showed normal histomorphology in all groups. Furthermore, the blood was collected from mice for BRT and BBT (Tables S1 and S2). As demonstrated, no obvious toxicity was found in groups treated with EZH2si-DMC complexes.

Discussion

Many gene mutations could cause cell proliferation, angiogenesis, tumor immunogenic abnormality and metastasis, leading to human tumorigenesis, which has been one of the

greatest threats to human health.^{19–22} Although the understanding of the molecular mechanisms of tumorigenesis becomes more and more profound, many malignant tumors are still resistant to traditional therapies. Recently, the definition of tumor-related genetic mutations has increased interest in cancer therapy and become the target of gene therapy.^{23–25}

A series of evidence suggests that EZH2 overexpression plays an important role in the development of tumors. Early studies have shown that overexpression of EZH2 is closely related to the malignant progression of prostate cancer. The same phenomenon has also been found in breast cancer, bladder cancer, melanoma, glioma, etc.^{26–28} The study also found that EZH2 overexpression is closely related to tumor initiation, development, progression, metastasis and drug resistance. Therefore, downregulation of EZH2 could effectively inhibit tumor growth and proliferation.

There are many ways to inhibit EZH2 activity, for example, shRNA, siRNA and small molecule inhibitors. ShRNA is a plasmid system, and it is difficult to use non-viral vector to deliver it to cell as the low transfection efficiency. The transfection efficiency could be high through viral vector system, but the security is very worrying. Small molecule

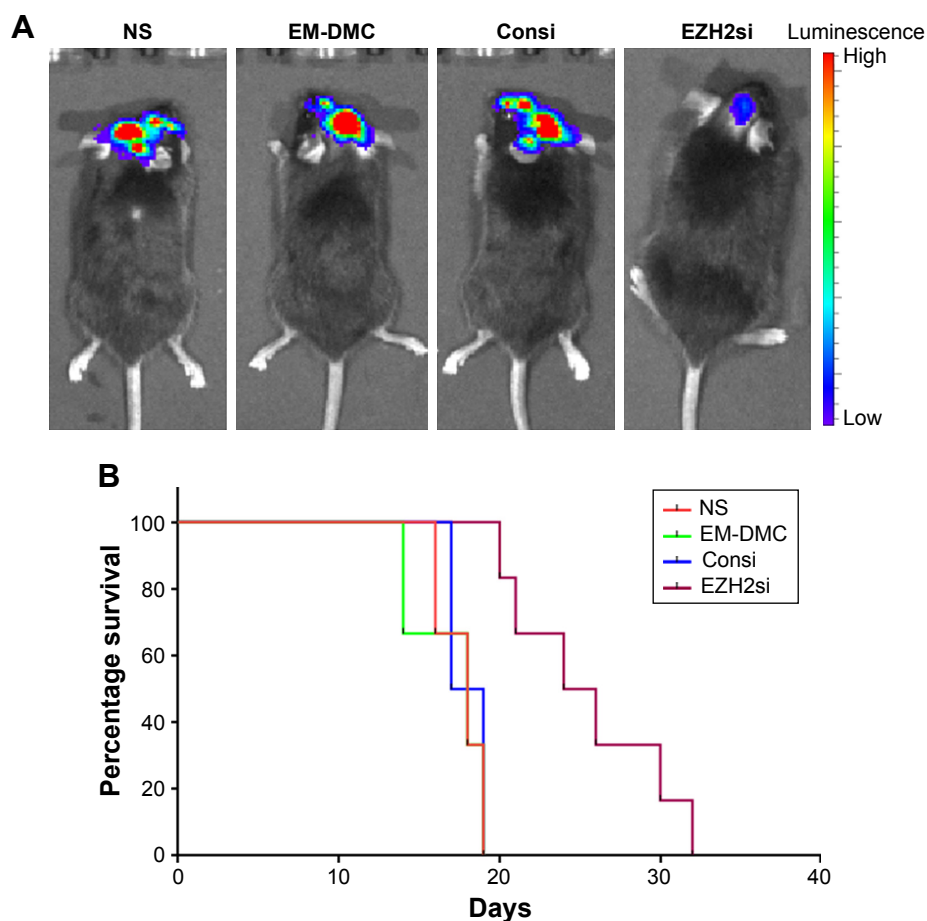


Figure 8 Bioimaging analysis in the GL261 orthotopic mice model.

Notes: (A) Intracerebral glioma was seen by using fluorescence markers. Tumor was inhibited more effectively by α -MM, compared with other groups. (B) Life survival time assessment. Both α -M and α -MM extended life spans of mice, while mice in the α -MM group reached a longer survival time.

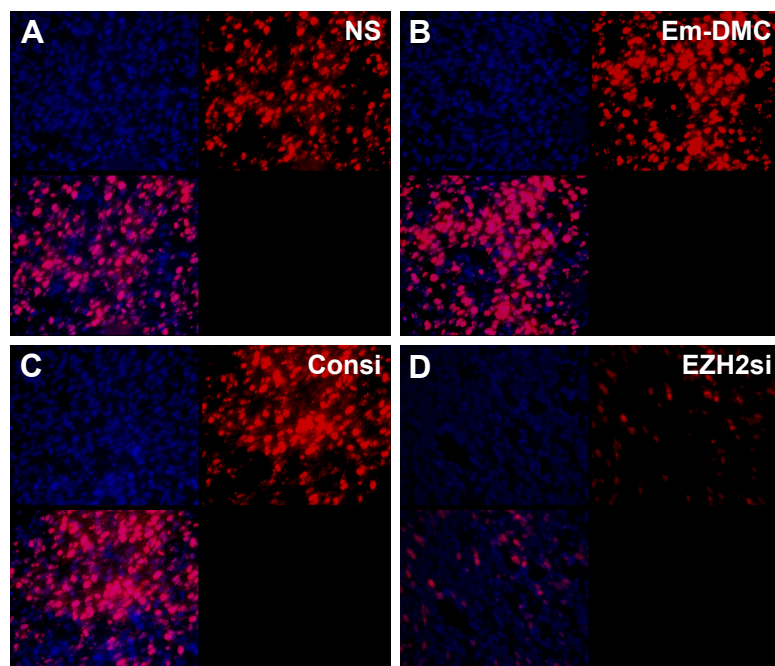


Figure 9 EZH2 expression detection in vivo.

Notes: (A) Intracerebral glioma was seen by using fluorescence markers. Tumor was inhibited more effectively by DMC-EZH2si complex, compared with other groups. (B) Life survival time assessment. DMC-EZH2si complex extended life spans of mice. The EZH2 expression of NS (A), DMC (B) and DMC-Consi (C) were higher than DMC-EZH2si (D). Results indicated that the EZH2 was successfully knocked down by the DMC-EZH2si complex.

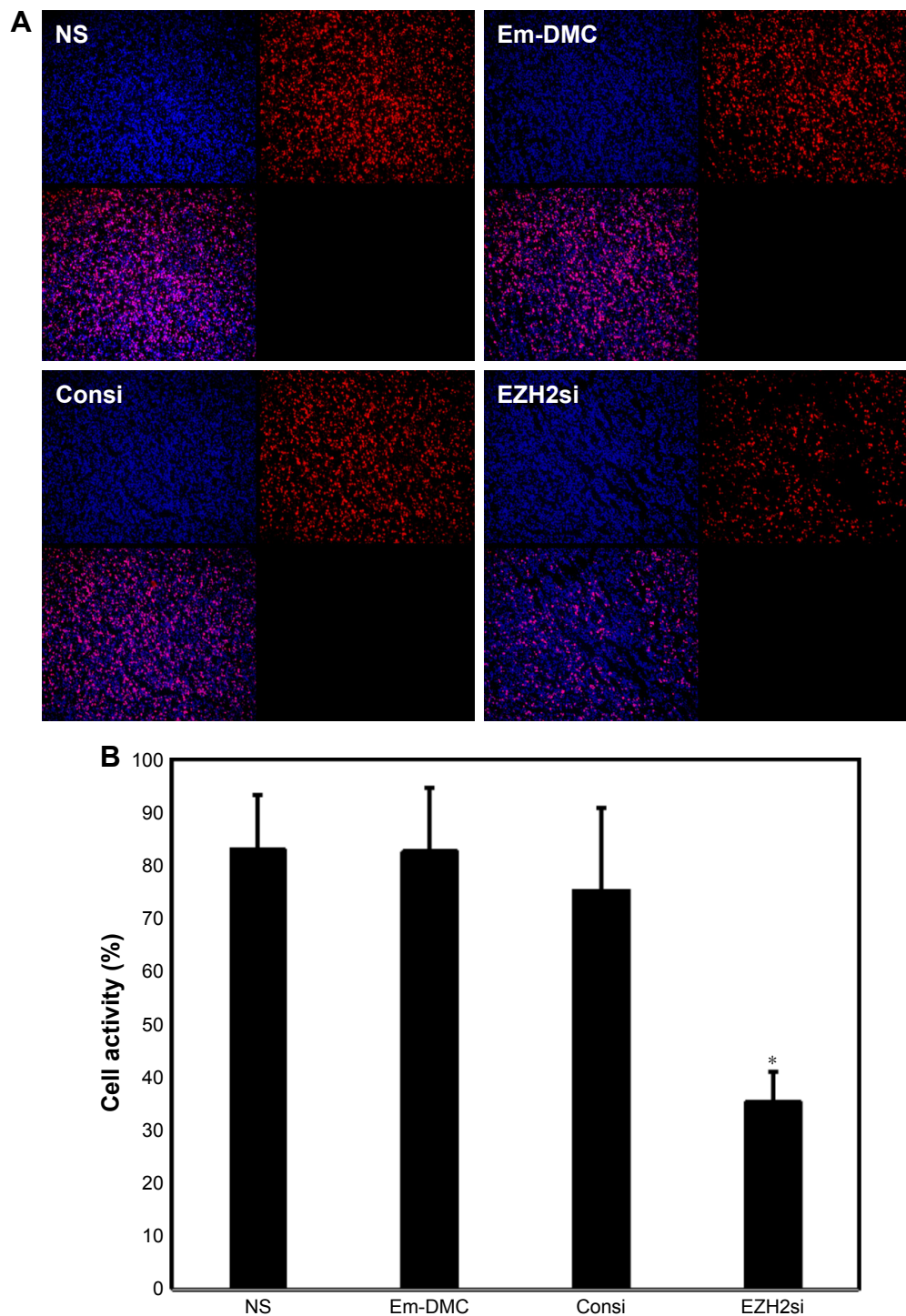


Figure 10 Cell proliferation detection.

Notes: (A) Cell proliferation was assessed by counting the number of Ki67-positive cells in the field (five high power fields per slide). (B) Mean cell proliferation every five fields was added. EZH2si-DMC was superior to other controls in inhibiting cell proliferation. EZH2si-DMC significantly inhibited cell proliferation. * $P < 0.01$, EZH2si-DMC versus NS, DMC, Consi-DMC.

inhibitors are relatively hot in recent years, but its specificity is not better. So, the siRNA system is a better method, which is safe and reliable because it is easy to use non-viral vector for transfection. Therefore, siRNA was designed to downregulate EZH2 protein for glioma treatment based on the target of EZH2. First, three different target RNA

sequences were designed to reduce the EZH2 protein level, and results showed that the third sequence of interference is most efficient. Then, the best siRNA was used in vivo to test the antiglioma effect. The results showed that siRNA/DMC could effectively inhibit the growth of glioma (EZH2si vs GS, EDMC and Consi/DMC, $P < 0.05$). Therefore,

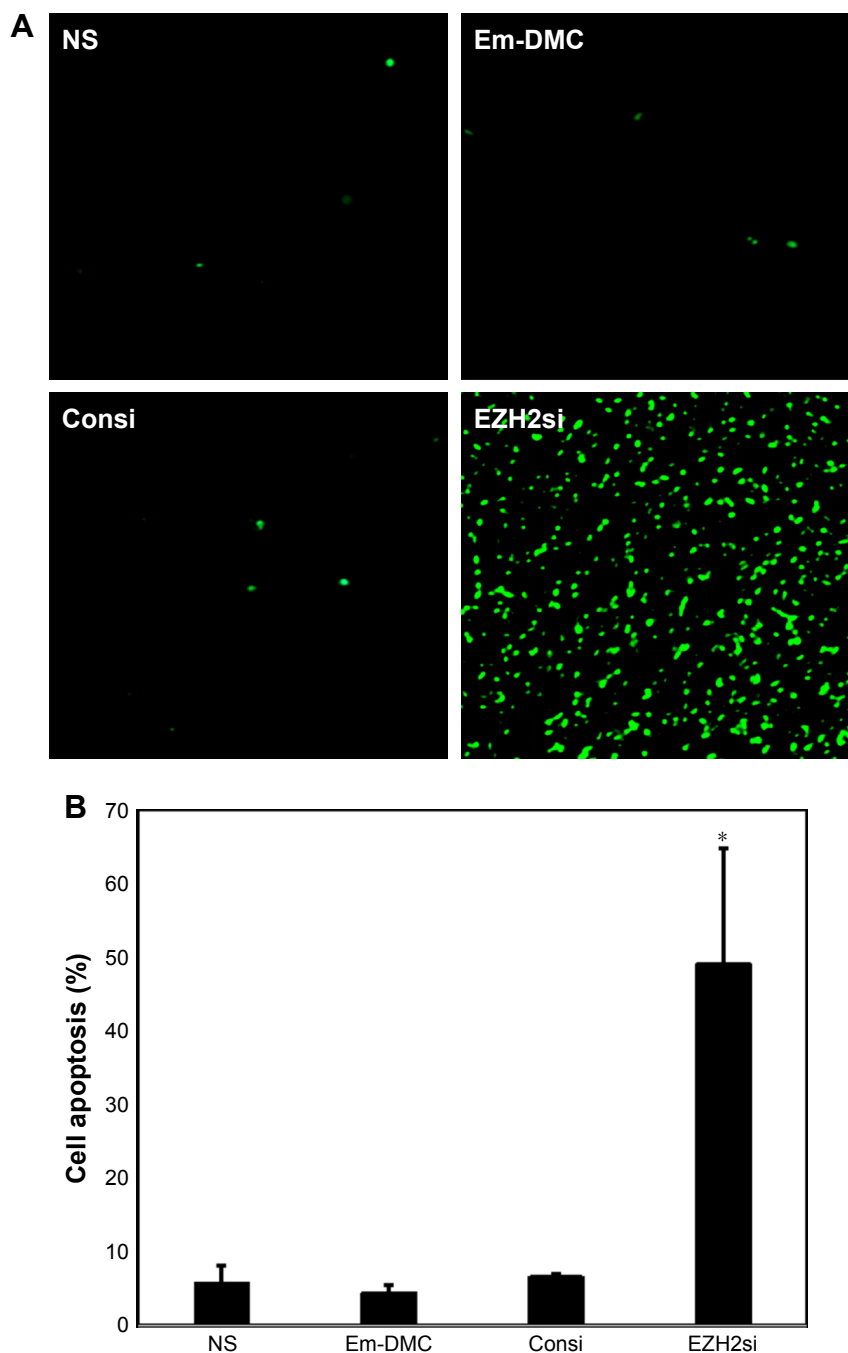


Figure 11 Cell apoptosis detection.

Notes: (A) Cell apoptosis was assessed by counting the number of TUNEL-positive cells in the field (five high power fields per slide), and EZH2si-DMC was superior to other controls in increasing cell apoptosis. (B) Mean apoptosis rate every five fields. EZH2si-DMC significantly increased apoptosis (* $P < 0.01$, EZH2si-DMC vs NS, DMC and Consi-DMC).

the nanoparticle gene vector was used to transport EZH2 siRNA in this work.

The therapeutic expectation of gene therapy is considerable because it has great potential of treating cardiovascular disease and certain autoimmune diseases caused by genetic defects and abnormalities (such as cancer, AIDS).^{29–32} Gene transfer or transfection is the basic technique for researching

gene function and protein expression in cells. Gene transfer is used for disease treatment, as it is intended to normalize the cells or even organs by introducing a gene encoding a functional protein into a cell to suppress a genetic disease.³³ Gene transmission is not only used to treat hereditary diseases but also for the production of a large number of secreted proteins for direct therapeutic applications or vaccine production.³⁴

It is well known that nucleic acids are difficult to pass directly through the plasma membrane because of the size and/or the physical and chemical properties, such as hydrophilicity. Various strategies have been developed for transporting nucleic acids, particularly genes. Ideal gene delivery and transfection systems should have high transfection efficiency and should be less toxic to cells and cell specific, while simultaneously handling heterogeneous systems with many different cells.

Although the virus system and physical methods aroused high attention by the researchers, they also have many shortcomings such as security.^{35,36} In order to overcome these shortcomings, various chemical transfection systems have been developed since the late 1960s, such as calcium phosphate, lipid and cationic polymers, including polyamide amine dendrimers and PEI, etc.^{37,38} The chemical gene delivery system is considered an alternative to viral gene vectors to avoid some of the problems associated with viral systems. In order to increase the efficiency of gene transfer and minimize the toxicity of these chemical transfection reagents, many great efforts such as regulating molecular structures and other features, including size, surface potential, have been made by the scientist.

In vitro, we successfully prepared a nanoparticle gene vector with a size of 50 nm and a potential of 36 mV. The siRNA was successfully encapsulated at a weight ratio of 50:1. Cell transfection experiments revealed that the vector was able to successfully transmit siRNA into glioma cells. The transfection efficiency was up to 95%. Therefore, the vector was used to transmit EZH2si, and it successfully knocked down the EZH2 from RT-PCR and Western blot tests.

In the previous study, EZH2 was proved to promote tumor cell proliferation, inhibit cell apoptosis and promote tumor growth.³⁹ In this study, knockdown of EZH2 in vitro could effectively inhibit the proliferation of glioma cells and induce glioma cell apoptosis, which is consistent with the previous study. In addition, apoptosis-related protein expression was detected, and the result indicated that depression of EZH2 can upregulate the pro-apoptotic protein Bax and downregulate the anti-apoptosis protein Bcl-2, which promoted cell apoptosis.

Conclusion

In this study, in order to research the further antitumor activity of DMC-EZH2si in vivo, the glioma subcutaneous tumor model was treated with DMC-EZH2si. The result showed that the glioma tumor is the smallest in the

DMC-EZH2si treatment group, indicating that DMC-EZH2si can effectively inhibit glioma growth in vivo. In addition, immunofluorescence experimental study found that DMC-EZH2si could inhibit cell proliferation and induce apoptosis in vivo to inhibit tumor growth. The results suggested that the DMC nanoparticle-mediated EZH2-siRNA may be a novel candidate for glioma therapy.

Acknowledgment

This work was supported by the National Natural Science Foundation of China (NSFC81502165 and NSFC81402240).

Disclosure

The authors report no conflicts of interest in this work.

References

- Verhaak RG, Hoadley KA, Purdom E, et al. Integrated genomic analysis identifies clinically relevant subtypes of glioblastoma characterized by abnormalities in PDGFRA, IDH1, EGFR, and NF1. *Cancer Cell*. 2010; 17(1):98–110.
- Phillips HS, Kharbanda S, Chen R, et al. Molecular subclasses of high-grade glioma predict prognosis, delineate a pattern of disease progression, and resemble stages in neurogenesis. *Cancer Cell*. 2006; 9(3):157–173.
- Mitchell DA, Batich KA, Gunn MD, et al. Tetanus toxoid and CCL3 improve dendritic cell vaccines in mice and glioblastoma patients. *Nature*. 2015;519(7543):366–369.
- Gerson SL. MGMT: its role in cancer aetiology and cancer therapeutics. *Nat Rev Cancer*. 2004;4(4):296–307.
- Kleer CG, Cao Q, Varambally S, et al. EZH2 is a marker of aggressive breast cancer and promotes neoplastic transformation of breast epithelial cells. *Proc Natl Acad Sci USA*. 2003;100(20):11606–11611.
- Nikoloski G, Langemeijer SM, Kuiper RP, et al. Somatic mutations of the histone methyltransferase gene EZH2 in myelodysplastic syndromes. *Nat Genet*. 2010;42(8):665–667.
- Xu K, Wu ZJ, Groner AC, et al. EZH2 oncogenic activity in castration-resistant prostate cancer cells is Polycomb-independent. *Science*. 2012;338(6113):1465–1469.
- Kouzarides T. Chromatin modifications and their function. *Cell*. 2007;128(4):693–705.
- Chang CJ, Yang JY, Xia W, et al. EZH2 promotes expansion of breast tumor initiating cells through activation of RAF1- β -catenin signaling. *Cancer Cell*. 2011;19(1):86–100.
- Lu C, Han HD, Mangala LS, et al. Regulation of tumor angiogenesis by EZH2. *Cancer Cell*. 2010;18(2):185–197.
- Richter GH, Plehm S, Fasan A, et al. EZH2 is a mediator of EWS/FLI1 driven tumor growth and metastasis blocking endothelial and neuro-ectodermal differentiation. *Proc Natl Acad Sci USA*. 2009; 106(13):5324–5329.
- Crea F, Fornaro L, Bocci G, et al. EZH2 inhibition: targeting the crossroad of tumor invasion and angiogenesis. *Cancer Metastasis Rev*. 2012;31(3–4):753–761.
- Fillmore CM, Xu C, Desai PT, et al. EZH2 inhibition sensitizes BRG1 and EGFR mutant lung tumours to TopoII inhibitors. *Nature*. 2015; 520(7546):239–242.
- Tachibana M, Amato P, Sparman M, et al. Towards germline gene therapy of inherited mitochondrial diseases. *Nature*. 2013;493(7434): 627–631.
- He Y, Cheng G, Xie L, et al. Polyethyleneimine/DNA polyplexes with reduction-sensitive hyaluronic acid derivatives shielding for targeted gene delivery. *Biomaterials*. 2013;34(4):1235–1245.

16. Wang CF, Lin YX, Jiang T, He F, Zhuo RX. Polyethylenimine-grafted polycarbonates as biodegradable polycations for gene delivery. *Biomaterials*. 2009;30(27):4824–4832.
17. Dai J, Zou S, Pei Y, et al. Polyethylenimine-grafted copolymer of poly(L-lysine) and poly(ethylene glycol) for gene delivery. *Biomaterials*. 2011;32(6):1694–1705.
18. Meng Y, Wang S, Li C, et al. Photothermal combined gene therapy achieved by polyethylenimine-grafted oxidized mesoporous carbon nanospheres. *Biomaterials*. 2016;100:134–142.
19. Bao X, Wang W, Wang C, et al. A chitosan-graft-PEI-candesartan conjugate for targeted co-delivery of drug and gene in anti-angiogenesis cancer therapy. *Biomaterials*. 2014;35(29):8450–8466.
20. She W, Luo K, Zhang C, et al. The potential of self-assembled, pH-responsive nanoparticles of mPEGylated peptide dendron-doxorubicin conjugates for cancer therapy. *Biomaterials*. 2013;34(5):1613–1623.
21. Wilson WR, Hay MP. Targeting hypoxia in cancer therapy. *Nat Rev Cancer*. 2011;11(6):393–410.
22. Huang Y, Goel S, Duda DG, Fukumura D, Jain RK. Vascular normalization as an emerging strategy to enhance cancer immunotherapy. *Cancer Res*. 2013;73(10):2943–2948.
23. Hill VK, Ricketts C, Bieche I, et al. Genome-wide DNA methylation profiling of CpG islands in breast cancer identifies novel genes associated with tumorigenicity. *Cancer Res*. 2011;71(8):2988–2999.
24. Li M, Zhang Z, Li X, et al. Whole-exome and targeted gene sequencing of gallbladder carcinoma identifies recurrent mutations in the ErbB pathway. *Nat Genet*. 2014;46(8):872–876.
25. Crowley E, Di Nicolantonio F, Loupakis F, Bardelli A. Liquid biopsy: monitoring cancer-genetics in the blood. *Nat Rev Clin Oncol*. 2013;10(8):472–484.
26. Matsika A, Srinivasan B, Day C, et al. Cancer stem cell markers in prostate cancer: an immunohistochemical study of Aldh1, Sox2 and EZH2. *Pathology*. 2015;47(7):622–628.
27. Li AM, Dunham C, Tabori U, et al. EZH2 expression is a prognostic factor in childhood intracranial ependymoma: a Canadian pediatric brain tumor Consortium study. *Cancer*. 2015;121(9):1499–1507.
28. Bracken AP, Pasini D, Capra M, et al. EZH2 is downstream of the pRB-E2F pathway, essential for proliferation and amplified in cancer. *EMBO J*. 2003;22(20):5323–5335.
29. Mckinney EF, Lyons PA, Carr EJ, et al. A CD8+ T cell transcription signature predicts prognosis in autoimmune disease. *Nat Med*. 2010;16(5):586–591. doi:10.1038/nm1951
30. Hacein-Bey-Abina S, Hauer J, Lim A, et al. Efficacy of gene therapy for X-linked severe combined immunodeficiency. *N Engl J Med*. 2010;363(4):355–364.
31. Klatzmann D, Abbas AK. The promise of low-dose interleukin-2 therapy for autoimmune and inflammatory diseases. *Nat Rev Immunol*. 2015;15(5):283–294.
32. Hinrichs CS. Molecular pathways: breaking the epithelial cancer barrier for chimeric antigen receptor and T-cell receptor gene therapy. *Clin Cancer Res*. 2016;22(7):1559–1564.
33. Yin H, Kanasty RL, Eltoukhy AA, et al. Non-viral vectors for gene-based therapy. *Nat Rev Genet*. 2014;15(8):541–555.
34. Schirmmacher V, Fournier P. Newcastle disease virus: a promising vector for viral therapy, immune therapy, and gene therapy of cancer. *Methods Mol Biol*. 2009;542:565–605.
35. Paul A, Hasan A, Kindi HA, et al. Injectable graphene oxide/hydrogel-based angiogenic gene delivery system for vasculogenesis and cardiac repair. *ACS Nano*. 2014;8(8):8050–8062.
36. Ni R, Zhou J, Hossain N, Chau Y. Virus-inspired nucleic acid delivery system: linking virus and viral mimicry. *Adv Drug Deliv Rev*. 2016;106(Pt A):3–26.
37. Lee MS, Lee JE, Byun E, et al. Target-specific delivery of siRNA by stabilized calcium phosphate nanoparticles using dopa-hyaluronic acid conjugate. *J Control Release*. 2014;192:122–130.
38. Kim H, Kim WJ. Photothermally controlled gene delivery by reduced graphene oxide-polyethylenimine nanocomposite. *Small*. 2014;10(1):117–126.
39. Bryant RJ, Cross NA, Eaton CL, Hamdy FC, Cunliffe VT. EZH2 promotes proliferation and invasiveness of prostate cancer cells. *Prostate*. 2007;67(5):547–556.

Supplementary materials

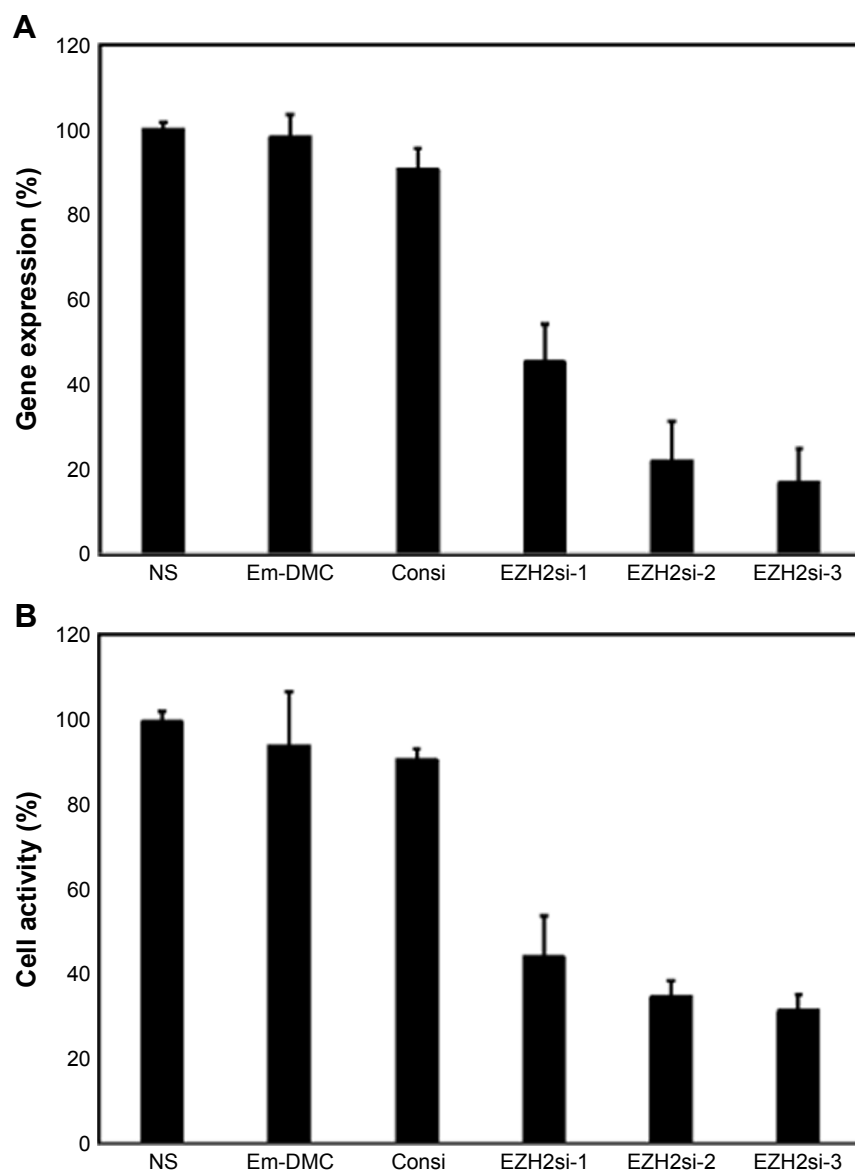


Figure S1 RT-PCR and MTT test of cell activity.

Notes: When GL261 cells were transfected with DMC, Consi-DMC or EZH2si-DMC for 72 hours, EZH2 expression was tested by RT-PCR (**A**) and cell activity was tested by MTT test (**B**). (siEZH2-1:GGATACAGCCTGTGCACAT; siEZH2-2:GCTTTGGACAACAAGCCTT; siEZH2-3:GCAAATTCTCGGTGTCAAA).

Abbreviation: RT-PCR, reverse transcription PCR.

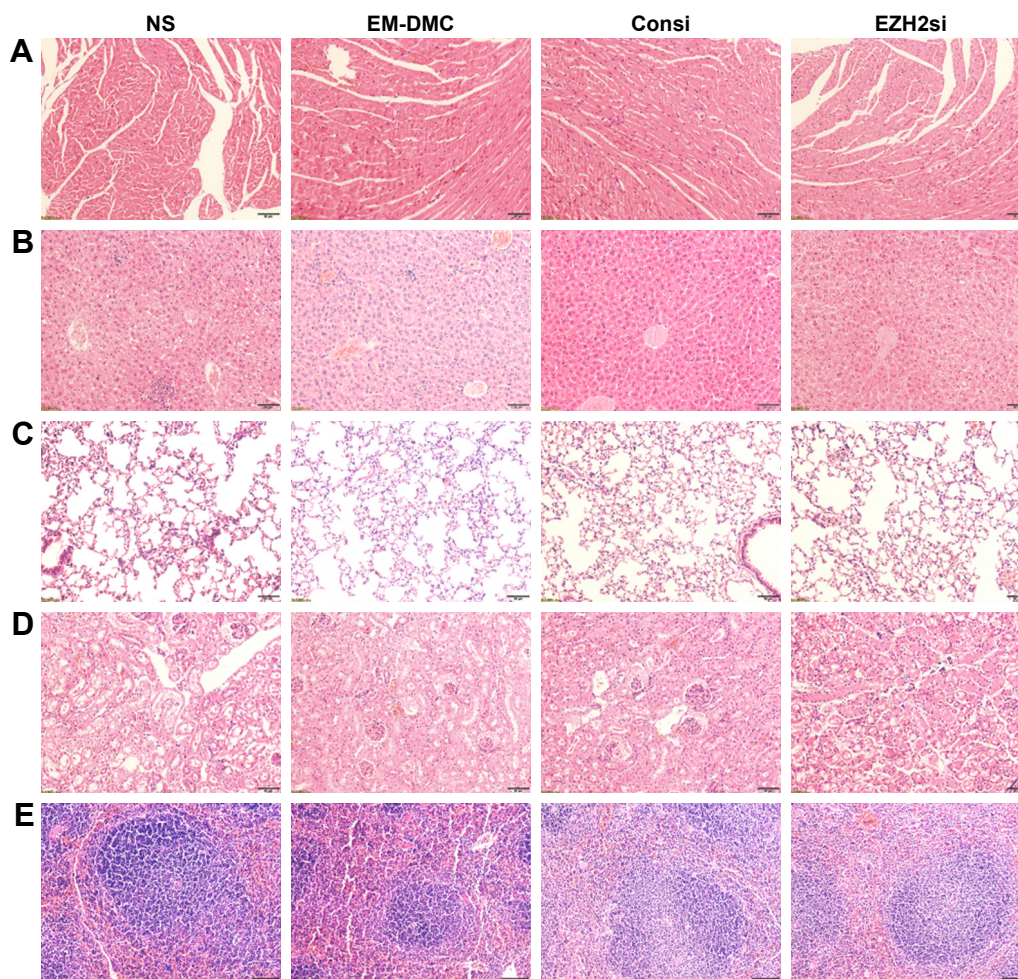


Figure S2 Toxicity assessment in vivo with pathological section.

Notes: Histological examinations of HE-stained (A) heart, (B) liver, (C) lung, (D) kidney, and (E) spleen. No significant pathological changes were detected. Scale bar is 50 μ m.

Table S1 Blood biochemical test

	ALB (g/L)	SEM	ALP (U/L)	SEM	ALT (U/L)	SEM
NS	23.7	0.3	81.4	3.7	27.0	5.7
EM-DMC	24.3	0.2	76.2	6.7	28.7	5.7
Consi	23.1	0.3	82.3	10.4	27.3	4.8
EZH2si	25.6	0.3	81.6	7.9	27.7	3.2
	AST (U/L)	SEM	BUN (μmol/L)	SEM	CHOL (mmol/L)	SEM
NS	277.3	0.4	8.2	1.2	2.7	0.1
EM-DMC	261	0.6	8.3	0.8	2.4	0.2
Consi	281.3	0.4	8.7	1.4	2.4	0.1
EZH2si	263.2	0.3	9.3	1.0	2.2	0.1
	CK (U/L)	SEM	CREA (μmol/L)	SEM	GLU (U/L)	SEM
NS	497.0	73.6	5.0	1.2	3.3	0.2
EM-DMC	516.7	67.2	4.8	0.6	3.2	0.3
Consi	501.0	135.4	4.3	1.3	3.7	0.1
EZH2si	497.3	6.3	4.1	0.7	4.1	0.3

(Continued)

Table S1 (Continued)

	HDL (U/L)	SEM	LDH (U/L)	SEM	LDL (mmol/L)	SEM
NS	1.1	0.1	1,679.67	277.8	0.2	0.01
EM-DMC	0.9	0.1	1,789.3	291.1	0.2	0.01
Consi	1.0	0.1	1,596.3	222.1	0.2	0.01
EZH2si	1.1	0.1	1,492.3	199.5	0.2	0.01
	TBIL (mg/dL)	SEM	TG (mmol/L)	SEM	TP (g/L)	SEM
NS	7.2	1.5	1.6	0.3	48.7	1.3
EM-DMC	7.1	1.3	1.5	0.3	50.1	1.2
Consi	7.2	1.1	1.6	0.2	51.8	2.0
EZH2si	8.0	1.2	1.7	0.2	51.7	1.8
	UA (μmol/L)	SEM	XAMY (U/L)	SEM		
NS	121.7	12.1	1,797.3	43.5		
EM-DMC	119.3	12.5	1,753.3	65.7		
Consi	114.7	10.7	1,877.0	102.7		
EZH2si	116.7	11.3	1,776.7	83.6		

Table S2 Blood routine test

Group	PLT ($10^9/L$)	SEM	RBC ($10^{12}/L$)	SEM
NS	319.7	96.8	9.5	0.1
EG	291.7	82.7	9.1	0.2
DM	307.7	61.7	9.3	0.2
DMG	311.3	33.0	9.5	0.2
	HGB (g/L)	SEM	WBC ($10^9/L$)	SEM
NS	170.7	9.2	7.6	1.2
EG	171.1	7.3	7.2	2.1
DM	163.0	8.6	7.4	0.9
DMG	170.0	16.5	7.6	1.2

International Journal of Nanomedicine

Dovepress

Publish your work in this journal

The International Journal of Nanomedicine is an international, peer-reviewed journal focusing on the application of nanotechnology in diagnostics, therapeutics, and drug delivery systems throughout the biomedical field. This journal is indexed on PubMed Central, MedLine, CAS, SciSearch®, Current Contents®/Clinical Medicine,

Journal Citation Reports/Science Edition, EMBase, Scopus and the Elsevier Bibliographic databases. The manuscript management system is completely online and includes a very quick and fair peer-review system, which is all easy to use. Visit <http://www.dovepress.com/testimonials.php> to read real quotes from published authors.

Submit your manuscript here: <http://www.dovepress.com/international-journal-of-nanomedicine-journal>